Theoretical and Experimental Study of Nonadiabatic Transonic Shock/Boundary-Layer Interaction

G. R. Inger*
Iowa State University, Ames, Iowa
and
F. T. Lynch† and M. F. Fancher‡
Douglas Aircraft Company, Long Beach, California

This paper describes a theoretical and experimental study of how surface heat transfer alters the local and global effects of a shock-wave/boundary-layer interaction (SBLI) on a nonadiabatic supercritical airfoil. In the presence of moderately strong but nonseparating local shocks typical of those encountered at supercritical wing cruising flight conditions, the present experiments show that even modest surface temperature differences above the adiabatic value cause significant drag increases and lift decreases that are much higher than observed under shockless subcritical conditions. A companion theory of the SBLI region agrees with pressure distribution data in the interaction zone and, indeed, predicts very significant increases in the displacement thickness and its interactive growth due to the increased wall temperature. A major reason for this effect is shown to be the large influence of heat transfer on the boundary-layer shape factor, to which SBLI is quite sensitive.

Nomenclature

C_f = skin friction coefficient, $=2\tau_w/\rho_{e_1}U_{e_1}^2$
C_p = pressure coefficient, $=2(p-p_\infty)/\rho_{e_1}U_{e_1}^2$
H_i = incompressible form factor, $=\delta_i^*/\Theta_i^*$
ℓ_u,ℓ_D = upstream and downstream influence distances
L = distance to shock location
M = Mach number
p = static pressure
p' = interactive pressure perturbation, $=p-p_1$
Δp = pressure jump across incident shock
Re_L = Reynolds number, $=\rho_{e_1}U_{e_1}L/\mu_{e_1}$
T = absolute temperature
u,v = velocity components in x,y directions
U_0 = undisturbed incoming boundary-layer velocity in x direction
x,y = coordinates along and normal to body surface
α = angle of attack
δ = boundary-layer thickness
δ^* = boundary-layer displacement thickness
Θ^* = momentum thickness
μ = ordinary coefficient of viscosity
ρ = density
τ = total shear stress

Subscripts and Superscripts

0 = undisturbed incoming boundary-layer properties
1 = inviscid flow conditions ahead of shock
AD = adiabatic wall conditions
e = conditions at boundary-layer edge
w = conditions at wall surface
∞ = freestream

Presented as Paper 83-1421 at the AIAA 18th Thermophysics Conference, Montreal, Canada, June 1-3, 1983; received Sept. 6, 1983; revision received Dec. 10, 1984.

*Glenn Murphy Professor, Department of Aerospace Engineering.
†Principal Staff Engineer, Aerodynamics Research and Development.
‡Senior Engineer Scientist, Aerodynamics Testing Technology, Research and Development.

Introduction

THE shock/boundary-layer interaction (SBLI) can have a significant local and global influence on supercritical transonic viscous flowfields.[1,2] The question as to how surface heat transfer can alter such interaction effects is relevant to the aerodynamics of models in the low-temperature nitrogen flow of a transonic cryogenic wind tunnel,[3] cooled turbine blades in hot-gas flows, the transonic supercritical flowfield around the hot post-re-entry Space Shuttle, and aerodynamic surface heating effects on the magnus moments acting on supercritical projectiles. This question was previously addressed in a preliminary theoretical study,[4] which suggested that even moderate nonadiabatic wall effects could be significant in these applications. The present work readdresses the problem more extensively for a representative aerodynamic flowfield that is of practical interest in its own right: the two-dimensional nonseparating transonic flow on a nonadiabatic supercritical airfoil. The goal is to achieve a better understanding of the heat-transfer effects, not only on the local SBLI zone, but also on the attendant global aerodynamics.

The local SBLI region is first analyzed by an extension of a successful[5,6] nonasymptotic triple-deck interaction theory to include the influence of small wall heat transfer ($T_w/T_{W,AD}=0.8$-1.2). This approach provides significant improvements on the earlier treatment,[4] the most important being that it allows for an arbitrary nonequilibrium shape factor value in the incoming turbulent boundary layer, which was found to be a major aspect of the heat-transfer effect on the SBLI zone and the subsequent downstream region. The experimental study, described subsequently, pertains to a typical supercritical airfoil with a detailed examination of the SBLI zone. The results verify the theoretical model and show that even a small heat transfer significantly influences the corresponding global aerodynamics.

Description of the Theoretical Approach

The Nonasymptotic Triple-Deck Model

Unlike significantly separated flow where the SBLI disturbance field involves a complicated bifurcated shock pattern, the unseparated case for turbulent boundary layers up to roughly $M_1\approx 1.3$ has a much simpler type of interaction pat-

tern that is amenable to analytical treatment.[5] In the practical Reynolds number range of interest here ($10^5 \leq Re_L \leq 10^8$), the local interaction disturbance field in the neighborhood of the impinging shock organizes itself into three basic layers or "decks" (Fig. 1): 1) an outer region of potential inviscid flow above the boundary layer, containing the incident shock and interactive wave system; 2) an intermediate deck of frozen shear stress/rotational inviscid disturbance flow occupying the outer 90% or more of the known incoming boundary-layer profile $M_0(y)$; 3) an inner shear disturbance sublayer adjacent to the wall that accounts for the interactive skin-friction perturbations (and hence any possible incipient separation), plus most of the upstream influence of the interaction. The forcing function of the problem here is thus impressed by the outer deck upon the boundary layer; the middle deck couples this to the response of the inner deck, but in so doing can itself modify the disturbance field to some extent; while the slow viscous/turbulent flow in the thin inner deck reacts very strongly to the pressure gradient disturbances imposed by these overlying decks.

In treating this interactive field a fully turbulent nonasymptotic theory[5] is employed that has been extensively validated by experimental data,[2,6] numerical studies with the full Navier-Stokes equations,[7] and basic analysis.[8] This approach provides at realistic Reynolds numbers a treatment of the inner deck pressure gradient terms plus the middle deck $\partial p/\partial y$ and streamline divergence effects, along with simplifying approximations that render the resulting theory tractable from an engineering standpoint. When the influence of shock obliquity at the boundary-layer edge is included,[2] extensive parametric studies and detailed comparisons with experiments on adiabatic bodies have shown that it gives a very good account of all the important engineering features of the interaction over a wide range of Mach and Reynolds number conditions. Moreover, the important but heretofore-ignored influence of incoming boundary-layer shape factor $\bar{H}_{i_1}$ (and hence the role of upstream pressure gradient, heat and mass transfer, and wall curvature histories) can be accounted for.

Heat-Transfer Effects on the Interaction

Under the continued stipulation of nonseparating two-dimensional turbulent interaction, two key assumptions about the heat-transfer aspects of the problem are introduced: 1) the wall temperature is essentially constant over the (short) length of the SBLI zone; and 2) only small amounts of heat transfer are present, as is often true in practice, characterized by values of $T_W/T_{W,AD}$ around unity (say, $0.8 \leq T_W/T_{W,AD} \leq 1.2$). Under such conditions, the basic triple-deck structure described above remains valid, with the thin inner deck still lying within the law of the wall region of the incoming turbulent boundary layer and the frozen turbulence approximation[5] still applicable to the middle deck.

Therefore, heat transfer can, in principle, influence the interactive flow in four ways: 1) by altering the outer inviscid disturbance flow and shock location via the global displacement thickness distribution; 2) by introducing new perturbation terms into the middle deck equations; 3) likewise adding such terms to the inner deck equation; and 4) by changing the incoming turbulent boundary-layer properties on which the interaction solution depends. Since the steady inviscid perturbation field is necessarily adiabatic, any influence of heat transfer resides solely in the global displacement effect of the underlying two decks on the inviscid shock location and strength. Since the present interaction theory describes perturbations *relative* to an assumed-known inviscid shock location, the first possibility is thus fully accounted for when one uses the aforementioned shock obliquity correction.

Regarding point 2, a detailed analysis was made of the middle deck interaction equations with eddy viscosity and conductivity perturbations neglected for an assumed inviscid-frozen turbulence flow. The results indicated that this disturbance field is in fact particle-isentropic along the streamlines, regardless of the heat-transfer rate across the incoming boundary layer; the corresponding perturbation equations therefore have exactly the same *form* as in adiabatic flow, with the heat-transfer effects fully accounted for by appropriate input values of the undisturbed boundary-layer Mach number, velocity, and density profiles in the coefficients.

Likewise, the inner deck question 3 has been carefully analyzed based on high Reynolds number laminar-turbulent shear disturbance equations including arbitrary compressibility and heat-transfer effects (see, e.g., Refs. 9 and 10 for details). Excluding extreme cases of hypersonic external flow, Prandtl numbers greatly different from unity and/or re-entry magnitudes of heat transfer, and provided the inner deck lies well below the sonic level of the incoming boundary layer (as it indeed does in practice), it was found that the influence of the small-density perturbation terms can be neglected and the disturbance flow taken as incompressible at all heat-transfer rates. Furthermore, it was found that heat transfer $\dot{q}_{w0}$ introduces only one significant new perturbation term due to the undisturbed flow density gradients acting on the streamwise pressure gradient perturbation, the coefficient of this term being directly proportional to the Nusselt number $\delta_{SL}\dot{q}_{w0}/C_p\mu_w$ based on the inner deck thickness δ_{SL}. However, since this coefficient can be shown to be extremely small in its effect (typically less than 1%) for the high Reynolds number/moderate heat-transfer conditions of interest here, this new term can be neglected and the inner deck disturbance equations taken in their usual (adiabatic) form with any heat-transfer effects accounted for by the coefficients.

Now, the properties[4] relevant to the interaction solution are the Mach number profile $M_0(y)$, the eddy viscosity and laminar sublayer damping functions in the wall region, and the overall values of skin friction C_{f_0}, displacement thickness δ_0^*, and shape factor H_{i_1}. Under the present small heat-transfer/low Mach number conditions, it is well known that the reference temperature method yields an accurate yet convenient and fundamentally based[11] determination of the nonadiabatic wall effect on these properties. When supplemented by the modified Crocco energy equation integral for the static temperature distribution plus the reference temperature version of Walz's composite law of the

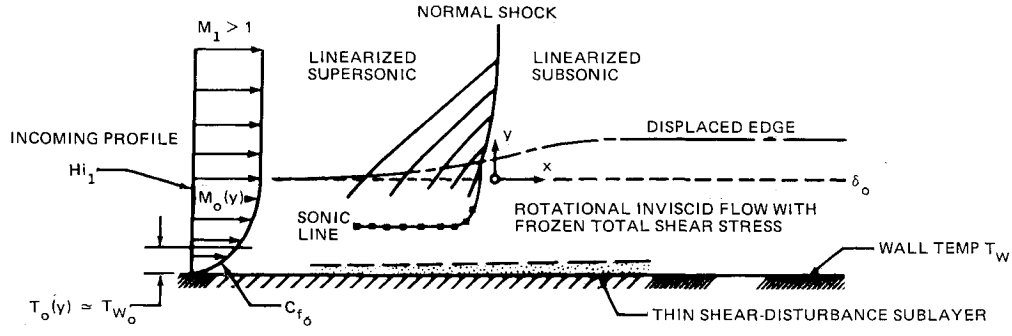

Fig. 1 Triple-deck structure of the local disturbance field in a nonseparating transonic SBLI.

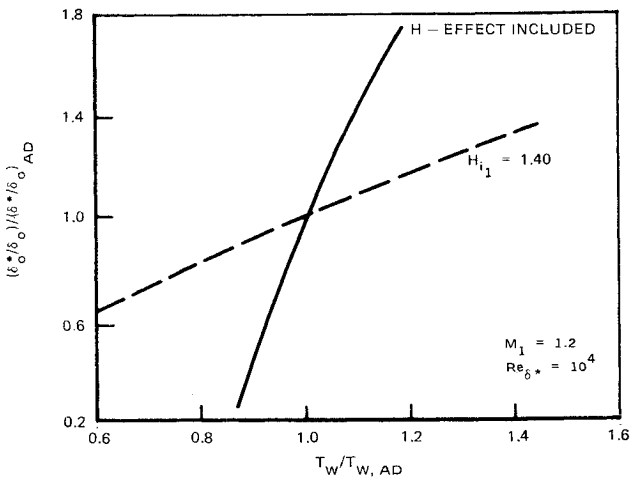

Fig. 2a Heat-transfer effect on noninteracted displacement thickness.

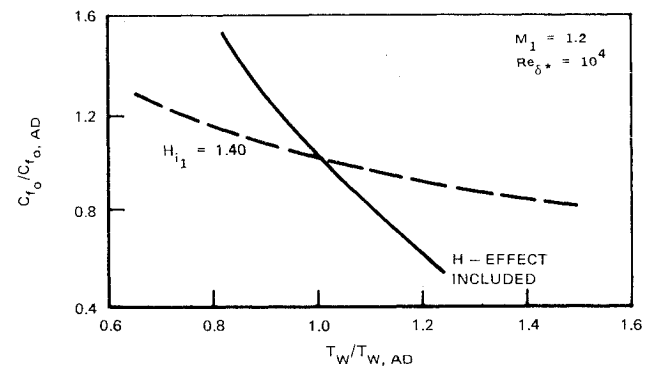

Fig. 2b Heat-transfer effect on noninteractive skin friction.

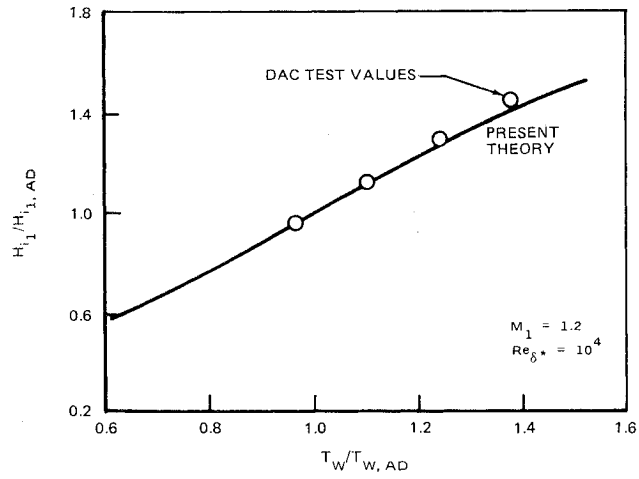

Fig. 2c Heat-transfer effect on incoming turbulent boundary-layer incompressible shape factor.

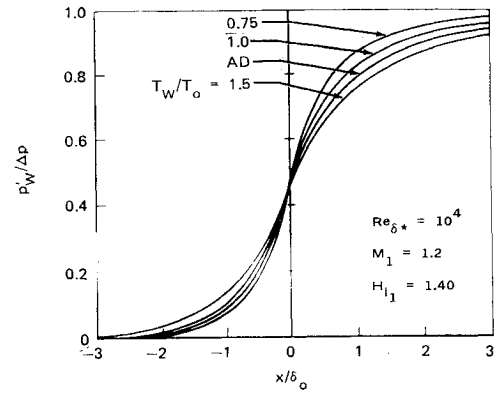

a) Wall temperature ratio effect (fixed H_{i_1}).

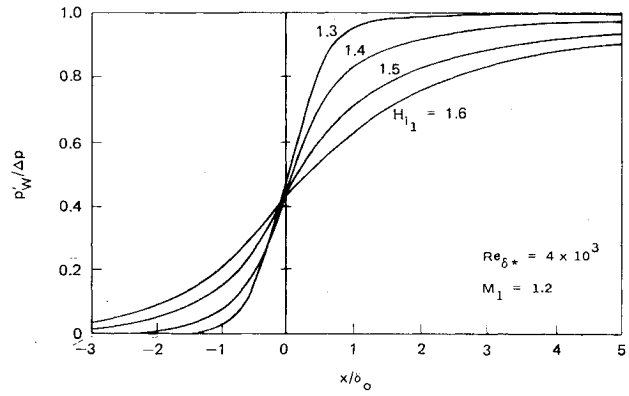

b) Influence of the shape factor.

Fig. 3 Typical heat-transfer effects on the interactive wall pressure distribution.

wall/wake velocity profile model[12] to determine $M_0(y)$, one has a complete and fully consistent first-order account of heat-transfer effects that can be readily implemented via straightforward modifications to Inger's existing[6] SBLI solution program.

This extended SBLI solution requires four independent input parameters: the preshock Mach number M_1, the boundary-layer displacement thickness Reynolds number $Re^*_{\delta_0}$, the incoming incompressible shape factor H_{i_1}, and the wall-to-edge temperature ratio T_W/T_e. An important advantage of this approach is that it allows arbitrary values of H_{i1} for the turbulent boundary layer and thus captures a significant effect of wall heat transfer through its influence on shape factor.

Parametric Study Results for the Influence of Heat Transfer

The typical predicted heat-transfer effect on the incoming undisturbed boundary layer is illustrated in Figs. 2a-2c, where the displacement thickness, skin-friction coefficient, and incompressible shape factor, respectively, are shown as functions of $T_W/T_{W,AD}$. The significant increase in δ_0^* and reduction in C_{f_0} with increasing wall temperature, plus their dramatic enhancement when the influence on shape factor is taken into account, are clearly seen, as is the appreciable increase of H_{i_1} with wall temperature. Note also here the agreement with the boundary-layer values obtained in the airfoil experiment (see below).

The predicted influence of heat transfer on the interactive pressure rise along the wall for a typical transonic flow case is shown in Fig. 3 in terms of both the explicit effect of the parameter T_W/T_e for a fixed shape factor (Fig. 3a) and the additional effect embodied in the shape factor (Fig. 3b). The latter effect is seen to be much more significant, causing an appreciable streamwise spreading out of the interaction region and weakening of $\partial p/\partial x$ with increasing wall temperature. This is brought out further in Fig. 4, which shows the theoretical upstream and downstream influence lengths (the distance ℓ_u ahead and ℓ_D behind the shock where the local pressure rise is 5 and 95%, respectively, of the overall shock pressure jump). When the shape factor effect is included, it is seen that even small amounts of heat transfer from the surface can double or triple ℓ_u, while tripling or quadrupling ℓ_D. Note that these conclusions involve the *ratio* of ℓ to the boundary-layer thickness (which itself depends on $Re^*_{\delta_0}$) and hence are not strongly dependent on Reynolds number; furthermore, the added ratioed manner of presenta-

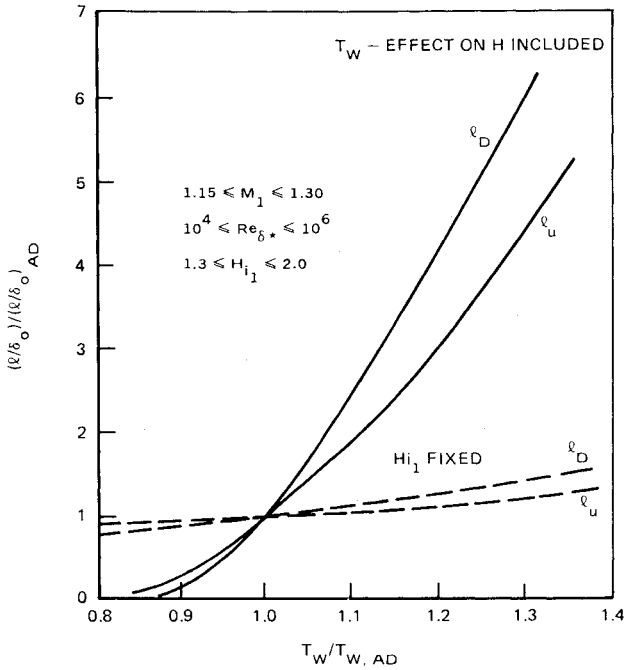

Fig. 4 Relative heat-transfer effect on the nondimensional streamwise interaction scales.

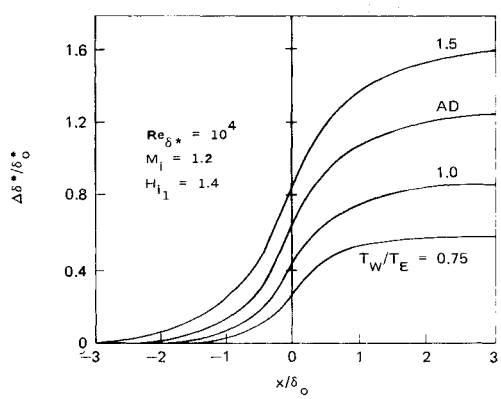

a) Wall temperature rate effect (fixed H_{i_1}).

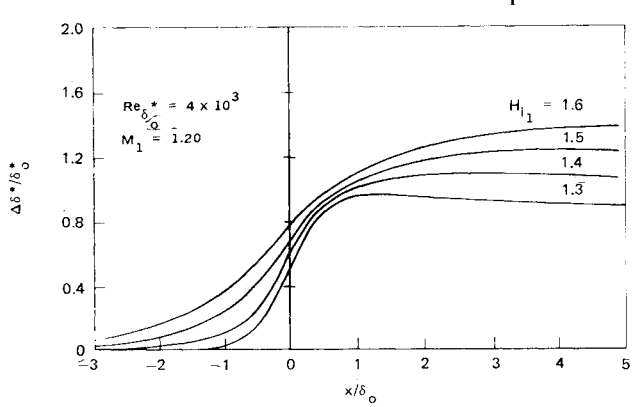

b) Influence of the shape factor.

Fig. 5 Typical heat-transfer effects on the interactive displacement thickness growth.

tion in Fig. 4 makes the results virtually independent of Reynolds number.

The corresponding heat-transfer effects on displacement thickness growth across the interaction zone are shown in Fig. 5, from which it is seen that the explicit effect of wall temperature is comparable to that of the shape factor: both cause an appreciable increase in the interactive thickening and its shock foot slope with T_W. This is further illustrated

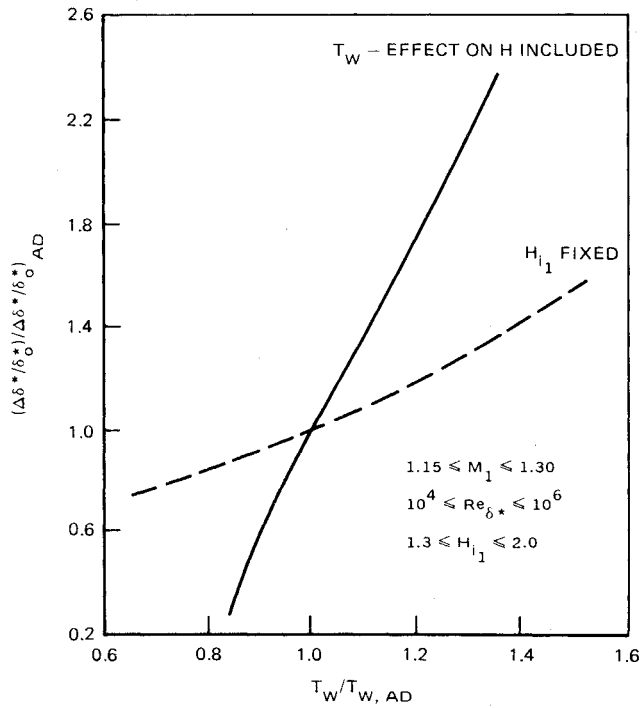

Fig. 6 Relative heat-transfer effect on the overall interactive displacement thickness increase.

in Fig. 6, where the overall increase in displacement thickness is plotted as a function of $T_W/T_{W,AD}$ in a ratioed manner that again renders the results virtually independent of Reynolds number.

Typical interactive skin-friction distribution predictions are shown in Fig. 7, where it is seen that the influence of heat transfer from a hot surface due to the direct wall temperature effect and the indirect effect on the shape factor both significantly reduce the local C_f throughout the interaction, this influence being least at the minimum value near the shock foot. Since in this regard the onset of local separation ($C_{f\min} \rightarrow 0$) is of particular importance, a parametric study of $C_{f\min}$ was carried out to determine the heat-transfer effect on the Mach/Reynolds number conditions where the incipient separation occurs. The results, presented in Fig. 8a, show that the explicit effect of increasing wall temperature hastens separation (i.e., it occurs at a lower M_1 for a given Reynolds number), as would be expected from Fig. 7. The additional implicit shape factor effect is in the same direction but weak, in agreement with experimental data[13] as indicated in Fig. 8b.

Experimental Study

Description of the Experiment

The heat-transfer data were obtained on a model of a nominally 14% thick supercritical airfoil in the transonic blowdown MDC 1 ft cryogenic wind tunnel (1-CWT). Instrumentation installed in the model included 80 static pressure taps distributed in chordwise rows at the centerline on the upper and lower surfaces, 38 pressure taps in spanwise rows, and 50 thermocouples installed to indicate surface temperature. A vertically oriented wake rake carrying seven static and seven total pressure probes and seven stagnation thermocouple probes was mounted on a strut behind the model, with the plane of the probes located 1.5 model chord lengths aft of the model trailing edge on the tunnel centerline (Fig. 9). The rake was traversed along the vertical axis.

Section lift coefficients were obtained by integration of the centerline chordwise pressure distribution and drag by integration of the momentum deficit of the wake. No signifi-

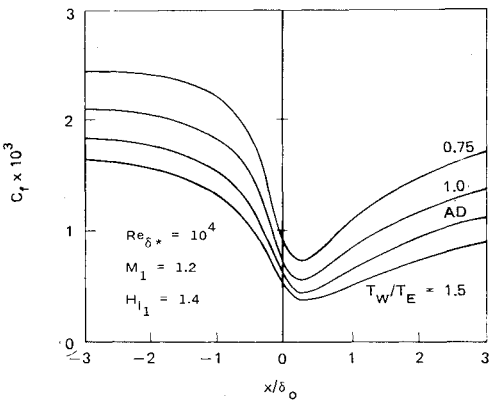

a) Wall temperature rate effect (fixed H_{i_1}).

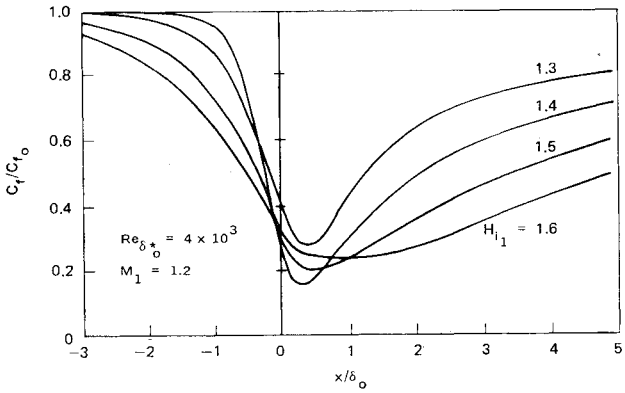

b) Influence of the shape factor.

Fig. 7 Typical heat-transfer effects on the interactive skin-friction distribution.

cant deviations from the two-dimensional flow were indicated in the spanwise pressure distributions at the reported conditions. Model static pressures were measured by a microprocessor-controlled electronic pressure scanning system using an individual solid-state transducer assigned to each model pressure station. Calibrations were automatically repeated both before and after each run. Each rake pressure was continuously measured by an individual transducer. Complete pressure surveys were accomplished in ~1 s, limited by the wake rake. Model wall temperature was determined from averages of measurements obtained from thermocouples located along the midspan of the model. Following installation in the model, all of the thermocouples were calibrated against a platinum resistance thermometer over the full range of the test temperatures in a cryostat. The adiabatic wall temperature for the experimental flows was calculated from the relation

$$T_{aw} = T_\infty \left[\frac{1 + 0.2M_\infty^2 (Pr_t)^{1/3}}{1 + 0.2M_\infty^2} \right] (1 + 0.2M_\infty^2) \qquad (1)$$

with assumed values of 1.4 for the ratio of specific heats and 0.86 for the turbulent Prandtl number, since the real-gas effects on the recovery factor were deemed negligible for the conditions of these tests.[14]

Initial model temperatures from ambient down to approximately 180°R were obtained by means of LN_2 spray nozzles located above and below the model. The 4 in. chord model was fabricated of beryllium-copper alloy to assure a uniform initial model temperature distribution. Heat-transfer data were obtained at a series of $T_W/T_{W,AD}$ ratios as the model temperature resolved toward the adiabatic condition at stable tunnel flow conditions. The model was maintained at a fixed geometric angle of attack during each run. Measurements

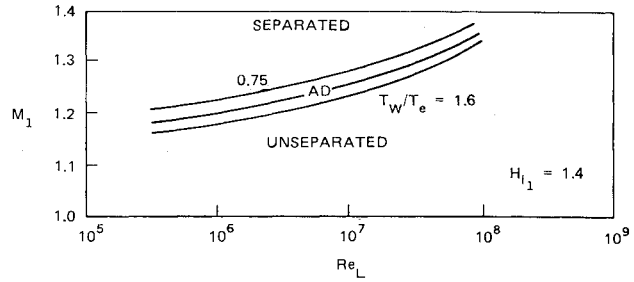

a) Wall temperature ratio effect.

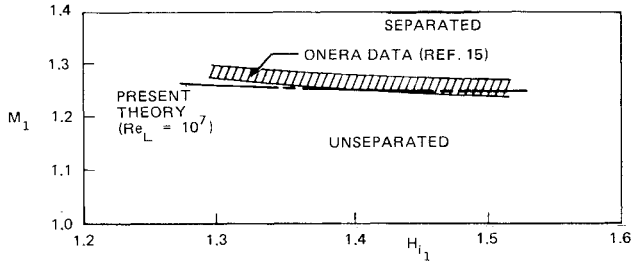

b) Shape factor effect.

'Fig. 8 Predicted influence of heat transfer on the conditions for incipient separation.

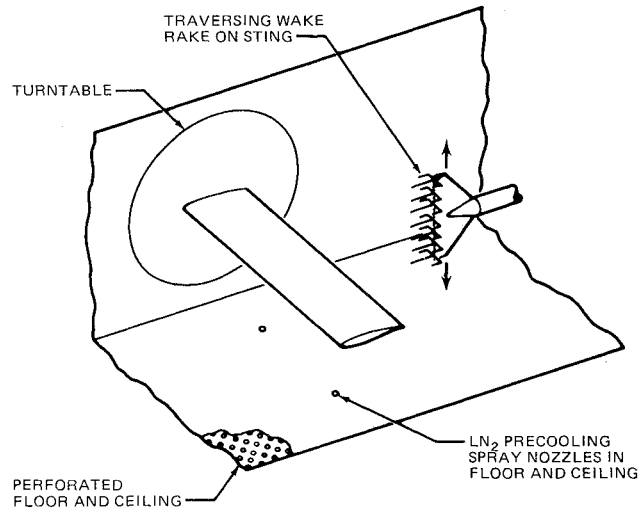

Fig. 9 Test section arrangement in 1-CWT.

were made for some free transition subcritical flows without shock waves and then for some important typical cruising condition cases for an airfoil/wing with transition fixed far forward where there is a shock wave on the upper surface that is never strong enough to cause separation at the shock (i.e., $M_1 < 1.3$).

Local Results in the SBLI Zone

Typical measured pressure distributions across the SBLI zone at two different supercritical flow angles of attack are presented in Fig. 10 for three different nonadiabatic wall temperatures at each angle; also shown for comparison are the corresponding predictions of the present interaction theory including the shock obliquity correction rule described in Ref. 2. It is seen that the overall interactive pressure rise is predicted reasonably well. More importantly, the predicted significant spreading out of the interactive pressure rise with the increased wall temperature, due to the effect on shape factor as discussed above, is corroborated to a large extent by the data, especially if one takes into account the indicated small experimental uncertainty in the shock location required to locate the SBLI predictions. However, the reason for the

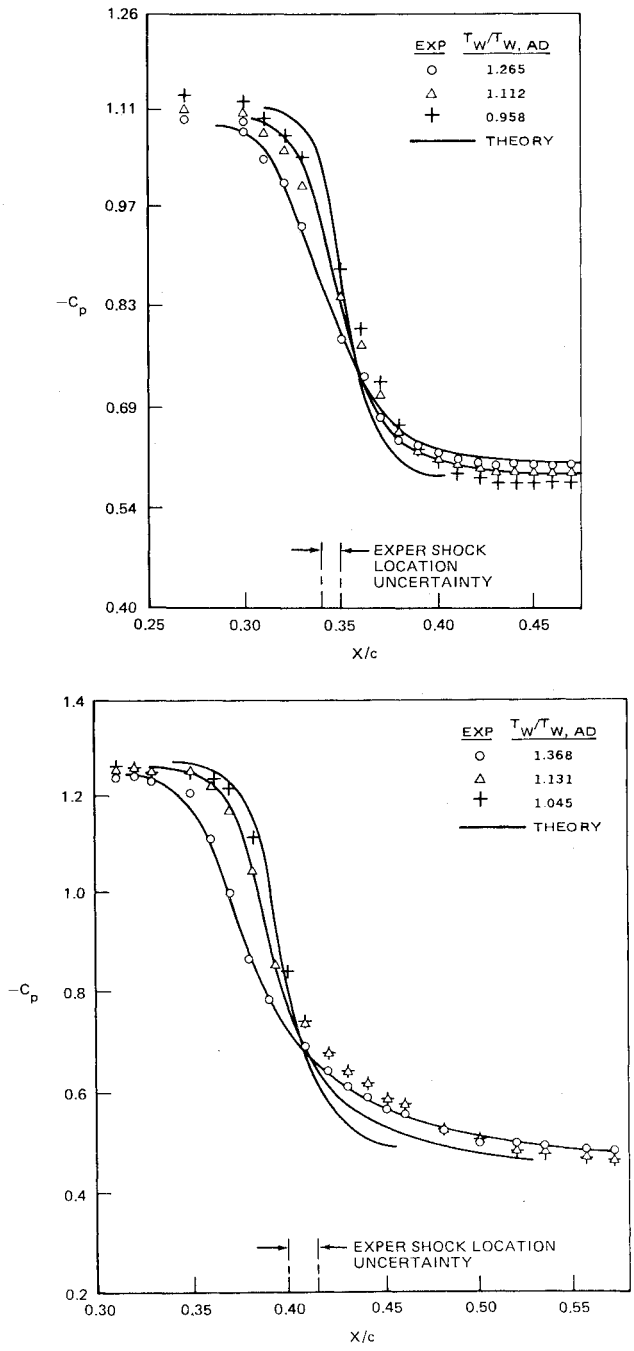

Fig. 10 Typical experimental and theoretical wall pressure distributions across the SBLI zone for various nonadiabatic surface temperatures ($M_\infty = 0.74$, $Re_c = 7.5 \times 10^6$): a) $\alpha = 4.75$ deg, b) $\alpha = 5.75$ deg.

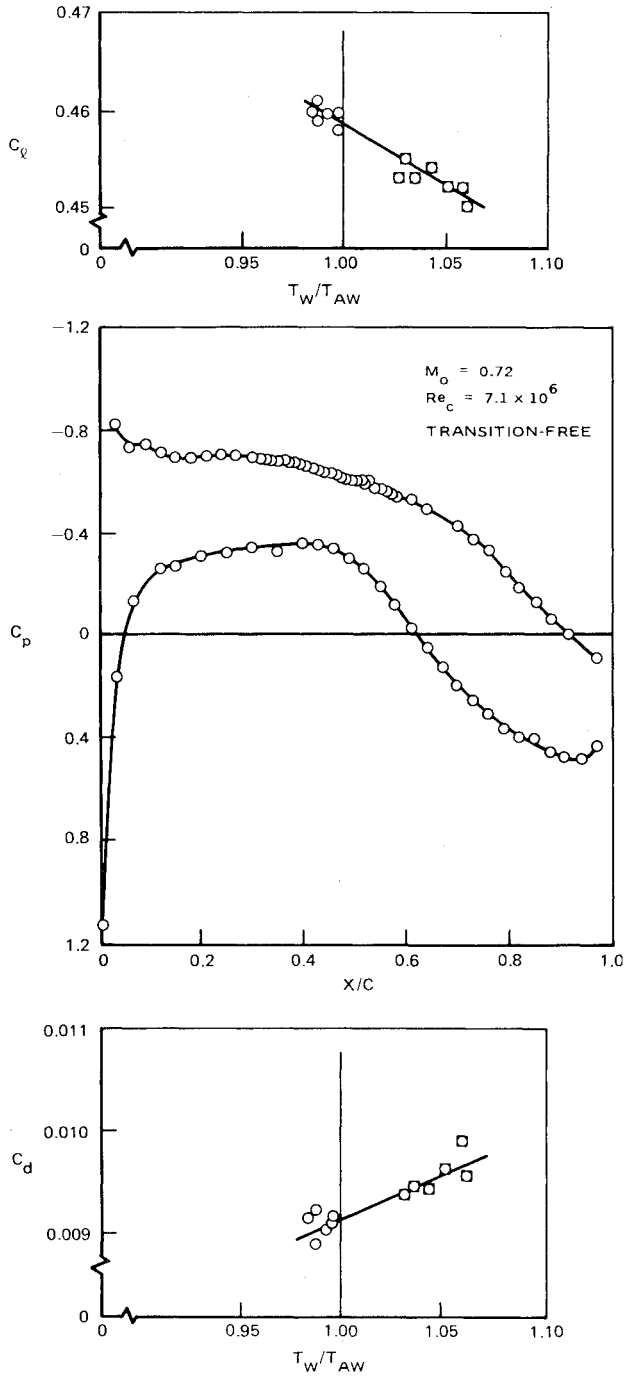

Fig. 11 Measured effects of nonadiabatic wall temperatures on total lift and drag for a typical subcritical case.

unusual long tail on the observed pressure distributions relative to the theory under these unseparated conditions at $M_1 \lesssim 1.25$ remains to be explained.

Another interesting feature of the experimental results observed in Fig. 10 is the forward movement of the shock with increasing wall temperature. Since the aforementioned general agreement of theory and experiment implies that the corresponding predicted displacement thickness effects (Figs. 3 and 6) are indeed occurring, this movement is ascribed to the large increase of both δ^* and its interactive growth with wall temperature.

Global Aerodynamic Results

Consider now the accompanying global aerodynamic forces that correspond to these local SBLI effects. As a basis of reference, Fig. 11 shows the effect of varying model surface temperatures on the measured lift and drag characteristics at transition-free conditions with a subcritical shock-free pressure distribution. It can be seen that the measured effects of wall temperature on lift and drag are quite small; for example, the drag coefficient change is about one count (0.0001) per percent deviation in surface temperature ratio from the adiabatic value.

More significant heat-transfer effects were observed, however, when a moderate strength nonseparating shock wave was present on the upper surface (i.e., $M_1 < 1.3$): the measured effect of varying the airfoil surface temperature on the measured lift and drag characteristics with transition fixed far forward on the airfoil is shown in Fig. 12 for such cruise cases with local Mach numbers at the shock of 1.24

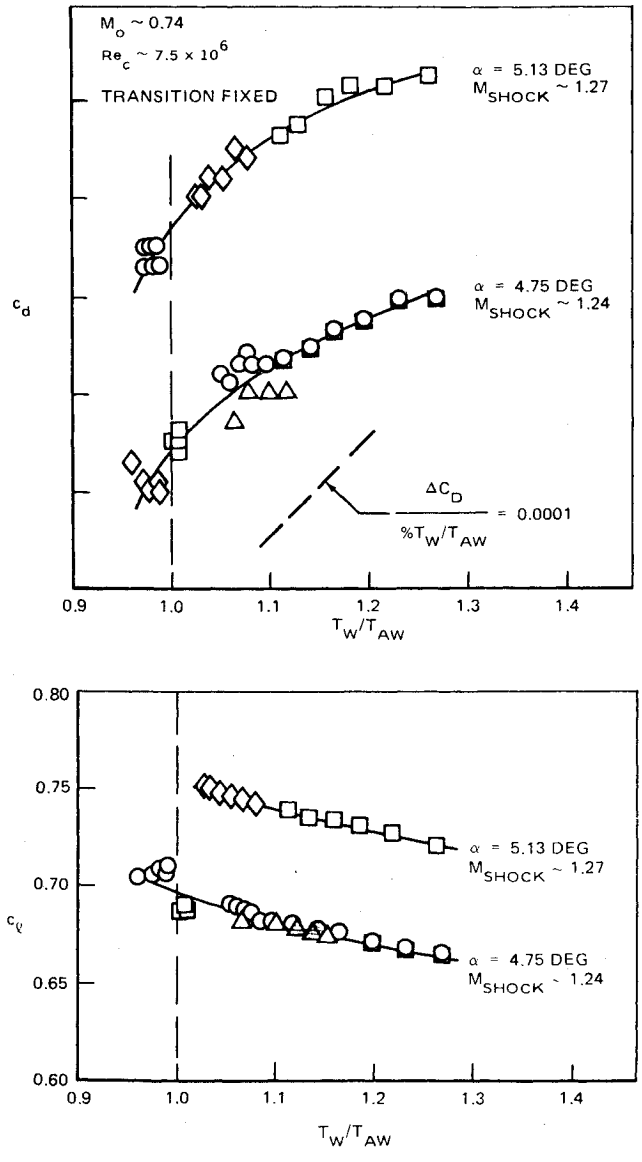

Fig. 12 Measured effects of nonadiabatic wall temperatures on lift and drag for several supercritical cases.

and 1.27. The measured drag change at a fixed angle of attack is close to one drag count (0.0001) per percent change in surface temperature ratio, accompanied by a change in lift coefficient of about 0.0015. From the aerodynamic testing viewpoint, this magnitude of drag sensitivity to deviations in surface temperature from the adiabatic value would dictate that the allowable deviation in temperature ratio from adiabatic conditions would be no more than 1% at the most. Regarding the perhaps surprisingly large corresponding C_ℓ reduction observed with increased wall temperature, it is noted that this is consistent with the enhanced displacement thickness growth and forward shock movement with the increasing T_W mentioned above.

Conclusions

In the presence of moderately strong but nonseparating local shocks typical of supercritical airfoil cruising flight conditions, the present experiments have shown that even modest surface temperature differences above the adiabatic value can cause significant drag increases and lift decreases that are much higher than observed under shockless subcritical conditions. A companion theoretical treatment of the SBLI region was also presented that generally agrees with pressure distribution data in the interaction zone and that indeed predicts very significant increases in the boundary-layer displacement thickness and its interactive growth due to increased wall temperature. The theory brings out that a major reason for this effect is the large influence of heat transfer on the boundary-layer shape factor, to which the SBLI behavior is quite sensitive. Among other things, these results strengthen an earlier suggestion[4] that the wall temperature ratio can be an important similitude parameter in the aerodynamic testing of supercritical airfoils and wings when viscous effects are of concern.

The present work implies that the influence of nonadiabatic wall temperatures may be even more significant for the strong shock supercritical flow conditions pertaining to buffet onset and/or maximum lift where shock foot or trailing edge region separation occurs. Further studies confirming this will be detailed in a subsequent paper.[15] On the basis of the study by Khan et al.,[16] even larger supercritical nonadiabatic effects may be expected at higher angle of attack flight conditions with larger-than-cruise lift coefficients.

References

[1]Inger, G. R., "Some Features of a Shock-Turbulent Boundary Layer Interaction Theory in Transonic Flow Field," *Computation of Viscous-Inviscid Interactions*, AGARD CP-291, 1980, pp. 18-1–18-66.

[2]Nandanan, M., Stanewsky, E., and Inger, G. R., "A Computational Procedure for Transonic Airfoil Flow Including a Special Solution for Shock-Boundary Layer Interaction," *AIAA Journal*, Vol. 19, Dec. 1981, pp. 1540-1546.

[3]Lynch, F. T. and Patel, D. R., "Some Important New Instrumentation Needs and Testing Requirements for Testing in a Cryogenic Wind Tunnel Such as the NTF," AIAA Paper 82-0605, March 1982.

[4]Inger, G. R., "Analysis of Transonic Shock Interaction with Nonadiabatic Turbulent Boundary Layers," AIAA Paper 76-463, July 1976.

[5]Inger, G. R., "Upstream Influence and Skin Friction in Non-Separating Shock Turbulent Boundary Layer Interactions," AIAA Paper 80-1411, July 1980.

[6]Inger, G. R., "Application of a Shock-Turbulent Boundary Layer Interaction Theory in Transonic Flowfield Analysis," *AIAA Progress in Astronautics and Aeronautics: Transonic Aerodynamics*, Vol. 81, edited by D. Nixon, AIAA, New York, 1982, pp. 621-636.

[7]Nietubicz, C., Inger, G. R., and Danberg, J., "A Theoretical and Experimental Investigation of a Transonic Projectile Flow Field," *AIAA Journal*, Vol. 22, Jan. 1984, pp. 35-43.

[8]Melnik, R., "A Survey of Turbulent Viscid-Inviscid Interaction Theory in Aerodynamics," AIAA Paper 84-0264, Jan. 1984.

[9]Lekoudis, S. G., Nayfeh, A. H., and Saric, W. S., "Compressible Boundary Layers Over Wavy Walls," *Physics of Fluids*, Vol. 19, April 1976, pp. 514-519.

[10]Inger, G. R., "Compressible Turbulent Boundary Layer Flow Past a Swept Wavy Wall with Heat Transfer and Ablation," *Astronautica Acta*, Vol. 17, 1971, pp. 325-338.

[11]Burggraf, O. R., "The Compressibility Transformation and the Turbulent Boundary Layer Equation," *Journal of the Aerospace Sciences*, Vol. 29, 1962, pp. 434-439.

[12]Walz, A., *Boundary Layers of Flow and Temperature*, MIT Press, Cambridge, Mass., 1969, p. 113.

[13]Sirieix, M., Delery, J., and Stanewsky, E., "High Reynolds Number Boundary Layer-Shock Wave Interaction in Transonic Flow," *Lecture Notes in Physics*, Vol. 148, Springer-Verlag, Berlin, 1982.

[14]Johnson, C. B. and Adcock, J. B., "Measurements of Recovery Temperature on an Airfoil in the Langley 0.3m Transonic Cryogenic Tunnel," AIAA Paper 81-1062, June 1981.

[15]Lynch, F. T., Fancher, M. F., and Inger, G. R., "Nonadiabatic Model Wall Effects on Transonic Airfoil Performance in a Cryogenic Wind Tunnel," *Wind Tunnels and Testing Techniques*, AGARD CP-348, 1983, pp. 14-1–14-11.

[16]Khan, M., Inger, G. R., and Lekoudis, S. G., "Computation of Transonic Flow Around Airfoils with Trailing Edge and Shock/Boundary Layer Interactions," *Journal of Aircraft*, Vol. 21, June 1984, pp. 380-388.